ARMY RESEARCH LABORATORY

Theoretical Studies of Solid Nitromethane

by Dan C. Sorescu, Betsy M. Rice,
and Donald L. Thompson

ARL-RP-14 February 2001

A reprint from the *Journal of Physical Chemistry B*, vol. 104, no. 35, pp. 8406–8419.

The findings in this report are not to be construed as an official Department of the Army position unless so designated by other authorized documents.

Citation of manufacturer's or trade names does not constitute an official endorsement or approval of the use thereof.

Destroy this report when it is no longer needed. Do not return it to the originator.

Army Research Laboratory
Aberdeen Proving Ground, MD 21005-5066

ARL-RP-14 **February 2001**

Theoretical Studies of Solid Nitromethane

Dan C. Sorescu
Oklahoma State University

Betsy M. Rice
Weapons and Materials Research Directorate, ARL

Donald L. Thompson
Oklahoma State University

A reprint from the *Journal of Physical Chemistry B*, vol. 104, no. 35, pp. 8406–8419.

Abstract

A classical potential to simulate the dynamics of a nitromethane crystal as a function of temperature and pressure is described. The intramolecular part of the potential was taken as superposition of bond stretching, bond bending, and torsional angles terms. These terms were parametrized on the basis of the geometric and spectroscopic (vibrational frequencies and eigenvectors) data obtained using ab initio molecular orbital calculations performed at the B3LYP/6-31G level on an isolated molecule. The intermolecular potential used is of the Buckingham 6-exp form plus charge–charge Coulombic interactions and has been previously developed by us (Sorescu, D. C.; Rice, B. M.; Thompson, D. L. *J. Phys. Chem.* 1997, B101, 798) to simulate crystals containing nitramine molecules and several other classes of nitro compounds. The analyses performed using constant pressure and temperature molecular dynamics simulations and molecular packing calculations indicate that the proposed potential model is able to reproduce accurately the changes of the structural crystallographic parameters as functions of temperature or pressure for the entire range of values investigated. In addition, the calculated bulk modulus of nitromethane was found in excellent agreement with the corresponding experimental results. Moreover, it was determined that the present potential predicts correctly an experimentally observed 45° change in methyl group orientation in the high-pressure regime relative to the low-temperature configuration. The analysis of the linear expansion coefficients and linear compression data indicate anisotropic behavior for the unit cell edges.

Theoretical Studies of Solid Nitromethane

Dan C. Sorescu, Betsy M. Rice, and Donald L. Thompson

Department of Chemistry, Oklahoma State University, Stillwater, Oklahoma 74078, and The U. S. Army Research Laboratory, Aberdeen Proving Ground, Maryland 21005

The Journal of
Physical Chemistry B®

Reprinted from
Volume 104, Number 35, Pages 8406–8419

Theoretical Studies of Solid Nitromethane

Dan C. Sorescu,[†,§] Betsy M. Rice,*[,‡] and Donald L. Thompson[†]

Department of Chemistry, Oklahoma State University, Stillwater, Oklahoma 74078, and The U. S. Army Research Laboratory, Aberdeen Proving Ground, Maryland 21005

Received: March 13, 2000; In Final Form: June 13, 2000

A classical potential to simulate the dynamics of a nitromethane crystal as a function of temperature and pressure is described. The intramolecular part of the potential was taken as superposition of bond stretching, bond bending, and torsional angles terms. These terms were parametrized on the basis of the geometric and spectroscopic (vibrational frequencies and eigenvectors) data obtained using ab initio molecular orbital calculations performed at the B3LYP/6-31G* level on an isolated molecule. The intermolecular potential used is of the Buckingham 6-exp form plus charge−charge Coulombic interactions and has been previously developed by us (Sorescu, D. C.; Rice, B. M.; Thompson, D. L. *J. Phys. Chem.* **1997**, *B101*, 798) to simulate crystals containing nitramine molecules and several other classes of nitro compounds. The analyses performed using constant pressure and temperature molecular dynamics simulations and molecular packing calculations indicate that the proposed potential model is able to reproduce accurately the changes of the structural crystallographic parameters as functions of temperature or pressure for the entire range of values investigated. In addition, the calculated bulk modulus of nitromethane was found in excellent agreement with the corresponding experimental results. Moreover, it was determined that the present potential predicts correctly an experimentally observed 45° change in methyl group orientation in the high-pressure regime relative to the low-temperature configuration. The analysis of the linear expansion coefficients and linear compression data indicate anisotropic behavior for the unit cell edges.

I. Introduction

This is the seventh in a series of papers describing our development and assessment of interaction potentials to be used in the study of dynamic processes in energetic materials. Our original intent was to develop a model to study nonreactive processes in the nitramine explosive RDX (1,3,5-hexahydro-1,3,5-*s*-triazine).[1] The potential that was developed consisted of atom−atom (6-exp) Buckingham potential terms plus electrostatic interactions. The Coulombic interactions were obtained through fitting atom-centered partial charges to a quantum-mechanically-determined electrostatic potential for a single RDX molecule whose structure corresponded to that in the crystal at ambient conditions. The remaining Buckingham parameters were adjusted to reproduce the experimental structure of the RDX crystal at ambient conditions. We found that this interaction potential could also describe the geometric parameters and lattice energies of different polymorphic phases of two other nitramine crystals: the polycyclic nitramine 2,4,6,8,10,12-hexanitrohexaazaisowurtzitane (HNIW, or CL-20)[2] and the monocyclic nitramine octahydro-1,3,5,7-tetranitro-1,3,5,7-tetraazacyclooctane (HMX).[3] Isothermal−isobaric molecular dynamics (NPT-MD) simulations for these crystals predicted cell parameters within a few percent of experimental values, and little translational or rotational disorder of the molecules. Further investigations to explore the limits of transferability of this interaction potential to other energetic molecular crystals were undertaken through performing molecular packing (MP) calculations for 30 nitramine crystals. These included several types of mono- and polycyclic nitramines, particularly crystals of importance in energetic materials.[4] For most of the crystals, the predicted structural lattice parameters obtained from molecular packing (MP) calculations differ by less than 2% from the experimental structures, with small rotations and practically no translations of the molecules in the asymmetric unit cell. A further assessment on the limits of transferability of the interaction potential was accomplished through molecular packing calculations of 51 crystals containing non-nitramine molecules with functional groups common to energetic materials.[5] MP calculations using this interaction potential reproduced the crystal structures to within 5% of experiment for these 51 non-nitramine systems, including the explosives pentaerythritol tetranitrate (PETN), nitromethane, 2,4,6-trinitrotoluene (TNT), and several nitrocubane derivatives.

More recently we have analyzed the dynamics of the important energetic crystals RDX, HMX, HNIW, and PETN under hydrostatic compression conditions using NPT-MD simulations and this intermolecular potential.[6] In that study we found that the predicted lattice parameters for the RDX, HMX, and HNIW crystals are in good agreement with experimental values over the entire range of pressures investigated experimentally. For the PETN crystal, the calculated crystallographic parameters were in acceptable agreement with experimental data for pressures up to 5 GPa. For higher pressures, the disagreements of predictions and experiment were attributed to the inadequacy of the rigid-body approximation used to simulate floppy molecules such as PETN.

The validity of the rigid molecular approximation was assumed in our previous studies.[1−6] As indicated by our results, this model has been very successful in its ability to describe

* Author to whom correspondence should be addressed.
† Oklahoma State University.
‡ The U.S. Army Research Laboratory, Aberdeen Proving Ground.
§ Current mailing address: Department of Chemistry, University of Pittsburgh, Pittsburgh, PA 15260.

10.1021/jp000942q CCC: $19.00
Published on Web 08/15/2000

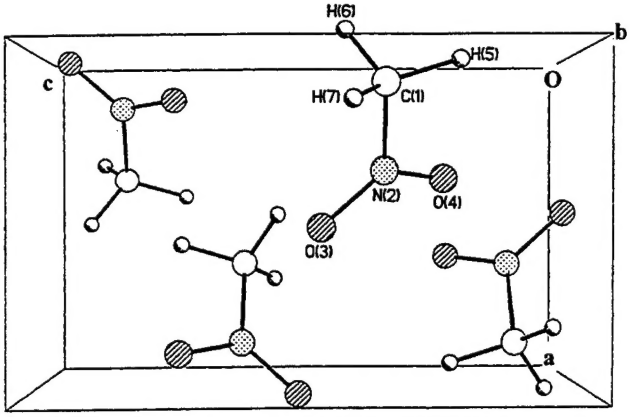

Figure 1. Representation of the nitromethane crystal unit cell with orthorhombic space group $P2_12_12_1$ and $Z = 4$ molecules per unit cell. Atom labels are consistent with the indices given in Table 1.

the equilibrium structures of a variety of organic molecular crystals under ambient conditions and with moderate increases in pressure and temperature. However, the physical and chemical processes of energetic materials that are of most interest occur within the regime of high pressures and temperatures, a regime in which conformational molecular changes become important. Consequently, further developments of the interaction potential are necessary to describe more realistically the intramolecular motion, molecular deformations, and the energy flow inside these crystals. For this purpose, in the present paper we eliminate the previously used rigid-molecule approximation[1-6] and extend the current intermolecular potential to include a full intramolecular potential for use in simulations of energetic materials. Particularly, in this work we consider the prototypical explosive, nitromethane.

Nitromethane was selected for our first attempt at developing a fully flexible model of an energetic molecular crystal since numerous experimental investigations of its properties under a wide range of conditions have been performed, thus providing significant data for use in assessing the model potential.[7-14] Single-crystal X-ray diffraction and neutron powder diffraction measurements indicate that the low-temperature structure of crystalline nitromethane belongs to the orthorhombic space group $P2_12_12_1$ with $Z = 4$ molecules in the unit cell (see Figure 1).[7] In this configuration the methyl group is in the staggered symmetric position with respect to the $C-NO_2$ plane. At ambient pressure, the crystal symmetry was observed to remain unchanged when the temperature was increased from 4.2 to 228 K.[7,9] In the temperature range 243−244 K an intermediate crystal phase (mesophase) was recently observed,[10] followed by transition to the liquid state at 244.73 K.[11] No crystallographic details have been provided about the intermediate phase at 243 K.[10]

The internal rotation of the methyl group in the crystal has received significant attention, since experimental evidence indicates that this motion is almost completely governed by intermolecular interactions. Analyses of the neutron powder diffraction patterns[7] for deuterated nitromethane at temperatures ranging from 25 to 125 K provided temperature-dependent amplitudes of librations of the methyl group about the C−N bond. Quasielastic neutron scattering spectra[8] recorded at temperatures ranging from 50 to 150 K are consistent with rotations of the methyl groups through 120° jumps rather than the 60° jumps observed in the gas phase. Furthermore, it was found[8] that in the crystalline phase the activation energy for the internal rotation of the methyl group is about 234 cal/mol, significantly higher than the corresponding gas-phase barrier of 6 cal/mol.[15] Inelastic neutron-scattering measurements[14] of tunneling splittings and of the lowest rotational states indicated that the methyl group activation barrier is significantly smaller than the energy of the second excited rotational state by ~170 cal/mol. These findings have been confirmed by infrared[16] and Raman[10] measurements, but the corresponding activation energies reported in these studies are slightly higher, namely 401 and 576 cal/mol, respectively. Several mechanisms have been proposed to contribute to the dynamics of methyl groups including the enhanced hopping due to interactions with phonons, band tunneling through thermally broadened excited states, or changes of the barrier with temperature.[14]

The influence of pressure on the internal rotational motion of the methyl group has also been examined. The crystal structure for isotropically compressed nitromethane has been determined through X-ray diffraction at pressures ranging from 0.3 to 15.3 GPa, at room temperature.[9,12] It was found that the space group and the packing arrangement remain unchanged relative to the low-temperature structure.[7] However, the measurements indicate a continuous change in the orientation of the methyl group with the increase of pressure. For pressures below 0.6 GPa the methyl group is freely rotating. At intermediate pressures (between 0.6 and 3.5 GPa) the rotation of the methyl group is hindered, while for pressures above 3.5 GPa the orientation of the methyl group becomes fixed. Moreover, it was determined that at pressures above 3.5 GPa, the methyl group is rotated by 45° relative to the low-temperature configuration.[7]

The ensemble of the above-presented experimental data provides many metrics against which to assess the performance of our interaction potential by molecular dynamics simulations. In this work, we describe such an assessment. In Section II, we provide a description of our potential model and our choice and parametrization of the intramolecular and intermolecular interaction terms. In Section III, we provide a brief description of computational details. Section IV contains the results of our MP and NPT-MD simulations and a comparison of predictions of crystal structural parameters with experimental values over a wide range of temperatures and pressures. Summary and conclusions are given in Section V.

II. Potential Energy Functions

We have assumed that the potential energy for a system of N nitromethane molecules can be described as the sum of inter- and intramolecular interaction terms:

$$V^{\text{total}} = \sum_{i=1}^{N}\left(V^{\text{intramolecular}} + \frac{1}{2}\sum_{j=1}^{N} V_{ij}^{\text{intermolecular}}\right) \qquad (1)$$

The intermolecular potential is the same as described in the earlier studies,[1-6] and consists of the superposition of a pairwise sum of Buckingham (6-exp) (repulsion and dispersion) and coulombic (C) potentials of the form:

$$V_{\alpha\beta}(r) = A_{\alpha\beta}\exp(-B_{\alpha\beta}r) - C_{\alpha\beta}/r^6 \qquad (2)$$

and

$$V_{\alpha\beta}{}^{C}(r) = \frac{q_\alpha q_\beta}{4\pi\epsilon_0 r} \qquad (3)$$

where r is the interatomic distance between atoms α and β, q_α and q_β are the electrostatic charges on the atoms, and ϵ_0 is the dielectric permittivity constant of free space. The parameters

TABLE 1: Force Field Parameters for Crystalline Nitromethane[a]

atom[b]	charge/e
C_1	−0.305342
N_2	0.820603
O_3	−0.470445
O_4	−0.484277
H_5	0.143365
H_6	0.155443
H_7	0.140652

Morse potential parameters

bond	D_e(kJ/mol)	β(Å^{-1})	r^0(Å)
C−N	251.0419414	2.005501	1.499574
N−O	390.3702976	2.459942	1.226747
C−H	426.7713101	1.892486	1.090000

bending potential parameters

angle	k_θ(kJ/mol rad^{-2})	θ(deg)
C−N−O	294.5211162	117.039960
O−N−O	657.8485114	125.890000
N−C−H	224.8140504	107.560708
H−C−H	149.9402928	111.312289

torsional potential parameters

angle	V_ϕ (kJ/mol)	δ(deg)	m
H_i-C_1−N_2−O_3 (i = 5,6,7)	0.27000 (0.49)[c]	−90.0	3.0
H_i-C_1−N_2−O_4 (i = 5,6,7)	0.27000 (0.49)[c]	90.0	3.0
N_2−O_4−O_3−C_1	240.37076	180.0	2.0

[a] The electrostatic charges have been determined by the CHELPG procedure as implemented in *Gaussian 94*[17] at the HF/6-31G** level. [b] The atom designation numbers are defined in Figure 1. [c] The choice of a torsional barrier of 0.49 kJ/mol is also discussed in text.

$A_{\alpha\beta}$, $B_{\alpha\beta}$, and $C_{\alpha\beta}$ for different types of atomic pairs have been previously published and have been used in the present study without change.[1]

The set of partial charges used in these calculations were determined through fitting these to the quantum-mechanically-derived electrostatic interaction potential for an isolated molecule whose atoms are arranged in the experimental crystallographic arrangement. These calculations have been done using the CHELPG procedure as implemented in the *Gaussian 94* package.[17] We have previously shown[4,5] that for the majority of the crystals studied, the best agreement between simulations and experiment occurs when the set of partial charges is determined using methods that employ electron correlation effects such as second-order Möller−Plesset (MP2) perturbation theory.[18] However, this was not true for nitromethane; the best agreement between the measured and the predicted crystallographic lattice parameters was obtained when unscaled partial charges derived from the Hartree−Fock (HF) wave function were used. The lack of improvement in the predicted lattice parameters when electron correlation effects are considered might be due to omission of other important interactions. These could include the omission of the polarization effects of neighboring molecules in the crystal when evaluating the electrostatic charges for the isolated molecule, or the assumption of a simple charge−charge interaction model when a multipolar interaction description would be more accurate. Nevertheless, our choice for the set of charges determined at the HF level (see Table 1), together with the rest of the potential parameters, give a very good representation of the crystallographic parameters.

In a previous study we have developed a complex intramolecular interaction potential to describe the unimolecular decomposition reactions of gas-phase nitromethane.[19] However, we do not require such a complex function in order to accomplish the goals described in this work. Thus, we have assumed a simpler form of the intramolecular interaction potential:

$$V^{\text{intramolecular}} = V_{\text{stretch}} + V_{\text{bend}} + V_{\text{torsion}} \tag{4}$$

to describe the bond stretching, angle bending, and torsional motions that occur within an isolated molecule. The bond stretches are represented by Morse potentials,

$$V_{\text{stretch}} = \sum_{i=1}^{6} D_{ei}\{\exp[-2\beta_i(r_i - r_i^0)] - 2\exp[-\beta_i(r_i - r_i^0)]\} \tag{5}$$

where r_i are the bond distances, D_{ei} are the bond dissociation energies, β_i are the curvature parameters, and r_i^0 are the equilibrium bond lengths. The six bond stretches that are described by this potential correspond to the six covalent bonds in nitromethane.

The bending potentials are represented by harmonic functions of the form

$$V_{\text{bend}} = \sum_{i=1}^{9} \frac{1}{2} k_i(\theta_i - \theta_i^0)^2 \tag{6}$$

where k_θ is the force constant and θ^0 the equilibrium value of the angle. The nine angles used to describe these interactions correspond to the HCH, HCN, CNO, and ONO angles in nitromethane.

Cosine-type torsional potentials have been used to describe the relative positions of the C−NO_2 atoms and the orientations of the H atoms relative to the C−N−O planes. The potentials have taken the form

$$V_{\text{torsion}} = \sum_{i=1}^{7} V_{\Phi i}[1 + \cos(m\Phi_i - \delta)] \tag{7}$$

where V_Φ is half of the intramolecular torsional barrier, Φ is the torsional angle, and $m = 2$ or 3. Six of the torsional angles used to describe these interactions correspond to HCNO angles, the seventh corresponds to the N−O−O−C torsional angle. The complete list of potential parameters from eqs 5−7 is given in Table 1.

The bond dissociation energies in eq 5 have been taken from our previous study of nitromethane in the gas phase,[19] while the remaining set of geometrical equilibrium values and force constants in eqs 5−7 were parametrized based on quantum mechanical information generated using density functional theory. These calculations have been done for the isolated molecule using Becke's three-parameter hybrid method,[20a] in combination with the Lee, Yang, and Parr correlation functional[20b] (B3LYP) and the basis set 6-31G*[21] using the *Gaussian 94* package of programs.[17] Our earlier molecular dynamics studies[22] on reactions of gas-phase energetic molecules suggested that a potential energy function fitted to only the structural parameters and normal-mode frequencies could lead to a model that produced anomalous and unexpected results, such as nonstatistical behavior in the unimolecular decomposition of the molecule. However, when the function was fitted to the ab initio Cartesian second derivatives of the energy, the potential model produced the expected statistical behavior in the unimolecular decomposition of the molecule. In this study, both the geometrical parameters of the optimized nitromethane molecule and

TABLE 2: Comparison between the Experimental, the Scaled Harmonic Vibrational Frequencies Calculated at B3LYP/6-31G*Level,[a] and the Predicted Frequencies by Our Force Fields; the Corresponding Projections (Scalar Product) of the Predicted Eigenvectors on the Ab Initio Eigenvectors Are Also Indicated[b]

	band type	ref 24a	ref 24b	ref 24c	ref 24d	ref 24e	B3LYP/6-31G*[a]	Mgas	Pgas	M1	P1	M2	P2
ν_t							51	50	0.94	117	0.94	157	0.94
ν_8	A_2''	476	477		480	475.2	461	459	0.99	461	0.99	461	0.99
ν_6	A_1''	599	605		607	602.5	584	596	0.94	601	0.94	605	0.94
ν_5	A_2'	647	658	656.0	655	657.4	636	602	0.92	605	0.92	605	0.92
ν_4	A_2'	921	918	917.1	917	917.9	892	828	0.93	821	0.92	821	0.92
ν_{11}	E''	1097	1087	1091.0	1103	1099.0	1076	1052	0.99	1053	0.99	1054	0.92
ν_{11}	E'	1153	1100	1146.0	1103	1119.0	1101	1098	0.99	1101	0.99	1103	0.99
ν_3	A_2'	1384	1377	1378.8	1379	1380.4	1364	1509	0.95	1508	0.95	1508	0.99
ν_2	A_2'		1397	1397.0	1402	1397.4	1388	1372	0.96	1368	0.96	1368	0.95
ν_{10}	E''	1449	1443		1426		1432	1432	1.00	1434	1.00	1437	0.99
ν_{10}	E'	1488	1482	1438.0	1426		1444	1434	0.99	1436	0.99	1439	0.99
ν_7	A_2''	1582	1586	1583.3	1561	1583.8	1615	1647	1.00	1618	1.00	1618	1.00
ν_1	A_2'	2965	2972	2964.3	2967	2973.9	2981	2961	1.00	2961	0.98	2961	0.98
ν_9	E''			2984.0	3045	3044.0	3070	3093	0.98	3093	1.00	3093	0.98
ν_9	E'	3048	3065	3080.4	3065	3080.0	3100	3095	0.98	3095	1.00	3095	1.00

[a] B3LYP/6-31G* values are scaled by 0.9613, as recommended in ref 23. [b] The columns denoted with Mgas, M1, and M2 correspond to the reference force fields for gas phase, for solid phase (with torsional HCNO barrier of 0.27 kJ/mol), and for solid phase with increased torsional barrier (torsional HCNO barrier of 0.49 kJ/mol), respectively. The corresponding projections of the predicted eigenvectors are indicated in columns Pgas, P1, and P2, respectively. The frequency units are cm^{-1}.

the ab initio eigenvalues (scaled by a factor of 0.9613[23]) and the corresponding eigenvectors of the ab initio Hessian matrix have been used in the fitting procedure.

Special attention was paid in this work to the choice of the torsional barrier V_Φ corresponding to the H−C−N−O torsional angles. As indicated in previous experimental studies,[8,10,14,16] an exact value for this barrier is not yet well-known and several values have been proposed. The major difficulties in determining a precise barrier for the internal rotation of the methyl group were due to the existence of a complex mechanism that incorporates enhanced hopping due to interactions with phonons, tunneling effects, and changes of the barrier with temperature. However, it is important to point out that independent of experimental technique used, the numerical values of the activation energy for the methyl rotation are quite small[8,10,16] and represent only fractions of 1 kcal/mol. In the present study we have investigated several values for V_Φ potential parameters of H−C−N−O torsions and have analyzed their role on the crystallographic parameters. The vibrational frequencies predicted by our classical potential for an isolated nitromethane molecule are given in Table 2 along with the corresponding ab initio values and experimental data. In this table we also indicate the values of the projections of the eigenvectors obtained from the normal-mode analysis using the proposed potential onto their quantum mechanical counterpart. A projection whose magnitude is one would indicate perfect agreement between the model and the B3LYP/6-31G* eigenvectors. A projection that has a magnitude near zero indicates that the atomic motion of the vibration that is predicted by the model is extremely different from that predicted by the quantum mechanical calculations. The projections of the normal-mode eigenvectors generated by different potential models (see below) onto the quantum mechanical eigenvectors are also indicated in Table 2.

In an initial attempt we described the internal methyl group rotational motion using a 6-fold torsional potential with a barrier of 6 cal/mol, in agreement with the experimental gas-phase barrier.[15] The vibrational frequencies corresponding to this model are indicated in Table 2 where they are denoted as Mgas. As can be seen there is an overall very good agreement between the entire set of predicted vibrational frequencies and the corresponding ab initio results. In particular, the frequency of the torsional mode ν_τ is practically identical to the corresponding quantum mechanical value. The corresponding projection of the eigenvector predicted by the model onto the quantum mechanical eigenvector is 0.94, indicating also a very good prediction of the vibrational motion associated to this mode. However, when this potential was tested in NPT-MD simulations in the regime of low temperatures and pressures it was found that while the unit cell size and shape of nitromethane were reasonably predicted, the methyl groups of the molecules in the unit cell were rotated by approximately 30° relative to the experimental orientation. This fact indicated the need to increase the barrier height of the torsional H−C−N−O potentials in order to reproduce accurately the crystallographic structure.

The second set of potentials we have considered is similar to the Mgas model but we have changed the HCNO torsional potential to a 3-fold form and increased the barrier parameter V_Φ(H−C−N−O) to 0.27 kJ/mol, which corresponds to an overall barrier for methyl rotation similar to that given in ref 14. The complete list of intramolecular parameters for this potential set is that indicated in Table 1. The modifications of the corresponding vibrational frequencies for this model are shown in columns denoted as M1 and P1 in Table 2. It can be seen that the most important variations of the vibrational frequencies take place for the mode ν_τ, which corresponds to the internal rotation of the methyl group. Overall, excepting modes ν_τ and ν_3 (which describes the inversion of the methyl group), there is good agreement between the predicted, the ab initio calculated, and the experimental[24] sets of vibrational frequencies with rms deviations of 6.9 and 10.8 cm^{-1}, respectively. In addition, the results indicate that the model reproduces the quantum mechanical eigenvectors very well, with the smallest projection values being 0.92 for modes ν_4 and ν_5. As will be described more fully hereafter, MP calculations and NPT-MD simulations using this potential model reasonably reproduce the experimental crystal structure and molecular conformations for the entire range of temperatures and pressures investigated. Consequently, all the results presented in the next sections correspond to this choice of potential parameters denoted as model M1.

A final choice of torsional potential parameters we have tested corresponds to an even larger value for V_Φ(H−C−N−O) of 0.49 kJ/mol. Our results indicate that this potential change has only a very small influence on the predicted crystallographic

TABLE 3: Lattice Parameters and Energies Obtained in Crystal Packing without Symmetry Constraints (the percentage change in lattice and molecular parameters after energy minimization is determined as a function of the experimental geometry and is given in parentheses)

	lattice energy[a]		lattice parameters[b]					
Q[c]	NB	ES	a	b	c	α	β	γ
EXP[d]								
	−52.3[e]		5.1832	6.2357	8.5181	90.000	90.000	90.000
LMIN								
20.5	−25.0401	−35.0560	5.2369	6.2653	8.6214	90.001	89.989	89.997
			(1.04)	(0.48)	(1.21)	(0.00)	(−0.01)	(0.00)
			Δx[f]	Δy	Δz	$\Delta\Phi$ (deg)[g]	$\Delta\Theta$ (deg)	$\Delta\Psi$ (deg)
			−0.037	−0.105	−0.014	3.44	3.02	6.41

[a] Nonbonded (NB) and electrostatic (ES) lattice energies per molecule in kJ/mol. [b] Lattice dimensions a, b, and c in angstroms, and angles α, β, and γ in degrees. [c] Cutoff parameter as described in text. [d] Experimental values from ref 7. [e] Estimated using the theoretical heat of sublimation of −47.3 kJ/mol as provided by Politzer.[34] [f] Change in fractional coordinates of molecular centroids for nitromethane molecule. [g] Change in Euler angles of molecular centroids for nitromethane.

parameters relative to the M1 model and that this influence is particularly limited to the region of low temperatures. Consequently we will make only limited references to this potential choice in the present work. For completeness, we indicate in Table 2 columns M2 and P2, the predicted vibrational frequencies and the corresponding projections for this potential model. As can be seen only the value of the torsional frequency ν_τ is increased by about 40 cm^{-1} relative to the M1 value while the projection of its eigenvector on the corresponding ab initio vector remains 0.94. The large value of this projection, close to unity, indicates that even for this high barrier value the model is representing correctly the corresponding vibrational atomic motions.

III. Computational Details

Molecular Packing Calculations. A first set of calculations used to test the semiempirical intermolecular potential energy functions proposed here is based on the use of molecular packing calculations,[25,26] in which the lattice energy of the crystal is minimized with respect to the structural degrees of freedom of the crystal. These calculations have been done using the algorithm proposed by Gibson and Scheraga[27] for efficient minimization of the energy of a fully variable lattice composed of rigid molecules and implemented in the program LMIN.[28] The nonbonded interactions were cut off with a cubic spline function from $P\sigma$ to $Q\sigma$, to ensure the continuity of the function and its first derivative. Here σ is the value of r in eq 2 at which $V_{\alpha\beta}(r) = 0$ and $dV_{\alpha\beta}(r)/dr < 0$. The parameters P and Q, which specify the start and the end of the cubic feather (see refs 1 and 27 for details), were set to 20.5 and 20.0, respectively. The coulombic potential terms of the form given in eq 3 are summed over the lattice using the Ewald technique as previously described.[1] Finally, the effect of pressure on the crystallographic parameters has been simulated by adding a potential term of the form $P(V - V_0)$,[27] where V_0 is the volume of a suitably chosen unit cell at zero pressure.

Constant-Pressure and -Temperature Molecular Dynamics Calculations. The dynamics of nitromethane as a function of temperature and pressure have been investigated using NPT-MD simulations based on the total potential described in eqs 1−7. For comparison we have also performed calculations using the rigid-body approximation[1−6] of the molecules in the system. In all simulations we have used the Nosé-Hoover thermostat−barostat algorithm[29] as implemented in the program DL_POLY_2.0,[30] to simulate the crystals at various temperatures and pressures. In this case, the equations of motion for molecules and the simulation cell are integrated using the Verlet leapfrog scheme.[31] In the case of rigid-molecules simulations the molecular rotational motion is handled using Fincham's implicit quaternion algorithm.[32]

The MD simulation cells consist of boxes containing 5 × 4 × 3 crystallographic unit cells. This choice of the simulation box ensures the use of a cutoff distance for the intermolecular potentials of about 10 Å. The initial configuration corresponding to the lowest temperature was chosen to be identical to that for the low-temperature experimental structure. The system was then equilibrated at that temperature and atmospheric pressure. In all production runs done using the Nosé-Hoover implementation for the NPT ensemble, the system was integrated for 34000 time steps (1 time step = .75 × 10^{-15} s), of which 4000 steps were equilibration. In the equilibration period, the velocities were scaled after every 5 steps so that the internal temperature of the crystal mimicked the imposed external temperature. Then, properties were calculated and accumulated for averaging over the next 30000 integration steps in the simulation. In subsequent runs, performed at successively higher temperatures or pressures, the initial configurations of the molecular positions and velocities were taken from the previous simulation at the end of the production run.

The lattice sums were calculated subject to the use of minimum-image periodic boundary conditions in all dimensions.[31] The interactions were determined between the sites (atoms) in the simulation box and the nearest-image sites within the cutoff distance. In these calculations, the coulombic long-range interactions were handled using Ewald's method.[31]

The main quantities obtained from these simulations were the average lattice dimensions and the corresponding volume of the unit cell. Additional information about the structure of the crystal has been obtained by calculating the radial distribution functions (RDF) between different atomic sites. Such quantities have been calculated from recordings done at every 10th step during the trajectory integrations.

IV. Results and Discussions

A. Molecular Packing Calculations. The results of MP calculations without symmetry constraints are presented in Table 3. As can be seen the predicted structural lattice parameters for nitromethane differ by less than 1.21% from the experimental values reported by Trevino et al.[7] Also, there are small translations but slightly larger rotations (with a maximum deviation of 6.4°) of the molecule in the asymmetric unit cell. Using the HF set of charges, the total lattice energy is predicted to be −60.1 kJ/mol. This value compares acceptably well with the lattice energy of −52.3 kJ/mol that has been estimated using

TABLE 4: Lattice Parameters Obtained in NPT-MD Calculations for Nitromethane as a Function of Temperature; the Calculated Thermal Expansion Coefficients (χ) at 250 K Are Also Indicated[a]

	lattice dimensions						
T(K)	a(Å)	b(Å)	c(Å)	α(deg)	β(deg)	γ(deg)	volume(Å^3)
4.2[b]	5.1832	6.2357	8.5181				275.3125
78.0[b]	5.1983	6.2457	8.5640				278.0476
228.0[b]	5.2440	6.3200	8.7300				289.3303
4.2	5.2116 (0.54)	6.3416 (1.69)	8.6464 (1.50)	89.998	89.999	90.000	285.7666 (3.79)
25.0	5.2134	6.3608	8.6935	90.012	90.018	89.996	288.3000
50.0	5.2184	6.3794	8.7266	90.001	90.034	90.000	290.5000
78.0	5.2195 (0.40)	6.4032 (2.52)	8.7543 (2.22)	89.991	89.996	89.991	292.5833 (5.22)
100.0	5.2222	6.4173	8.7734	90.001	89.962	90.007	294.0166
125.0	5.2267	6.4329	8.7979	89.987	89.994	90.002	295.8166
150.0	5.2298	6.4605	8.8204	89.974	89.991	90.010	298.0166
175.0	5.2373	6.4889	8.8606	89.995	90.005	89.987	301.1166
200.0	5.2452	6.5167	8.8808	90.016	90.012	90.020	305.3166
228.0	5.2534 (0.18)	6.5481 (3.60)	8.9195 (2.17)	90.015	90.020	90.043	303.5667 (4.92)
250.0	5.2620	6.5691	8.9561	90.001	89.993	89.946	306.8167
χ[c]	68.9×10^{-6}	181.7×10^{-6}	131.9×10^{-6}				380.5×10^{-6}

[a] The values in parentheses represent the percentage differences relative to the available experimental results. [b] Experimental data from ref 7. [c] The units for the linear and volume expansion coefficients are K^{-1}.

the relation $U_{lat} \approx -\Delta H_{subl} - 2RT$.[33] In this analysis we have used as the heat of sublimation for nitromethane the value of 47.2 kJ/mol estimated theoretically by Politzer.[34]

B. NPT-MD Calculations. NPT-MD simulations of nitromethane were used to predict the crystal structure of nitromethane over a large range of temperatures and pressures. We will first examine thermal effects on the crystallographic cell and molecular parameters at 1 atm, and compare them against experimental values.

B1. Temperature Effects. Average unit cell edge lengths and volumes determined from NPT-MD simulations for the flexible model for temperatures ranging from 4.2 to 250 K are given in Table 4. These data are represented in Figure 2, along with the corresponding experimental values and the NPT-MD results obtained using the rigid-body approximation. For the flexible model, the NPT-MD lattice dimensions obtained at $T = 4.2$ K are in very close agreement with those determined in the MP calculations and with the experimental values.[7] At this temperature, the percentage differences between the predicted and the experimental lattice dimensions are 0.54%, 1.69%, and 1.50% for the **a**, **b**, and **c** axes, respectively. The deviation of the predicted unit cell volume from the experimental value at this temperature is 3.79%. This good agreement is decreased only slightly with an increase in temperature. At $T = 78$ K, the cell edge lengths and the unit cell volume agree with the experimental values to within 2.52% and 5.22%, respectively. At the highest temperature where experimental data are available (228 K), the deviations from experiment for the cell edges are less than 3.60% while the difference is 4.92% for the unit cell volume. Also, the unit cell angles remain close to 90.0° for the entire temperature range analyzed, as expected for the orthorhombic symmetry of the crystal. For comparison, calculations using the M2 potential model indicate slightly larger deviations for the predicted lattice parameters from experimental values of 1.31%, 1.03%, and 1.72% at $T = 4.2$ K and 0.60%, 3.61%, and 2.13% at $T = 228$ K for the **a**, **b**, and **c** axes, respectively.

The linear and volume thermal expansion coefficients extracted from the data are also given in Table 4. The expansion of the lattice is highly anisotropic with the largest length changes along the **b** and **c** axes. These effects can be partially attributed to the internal rotation of the methyl group. To illustrate our argument, consider the limiting case in which a nitromethane molecule is arranged in a unit cell such that the C−N bond is parallel to the **a** axis. Changes in the positions of the hydrogen

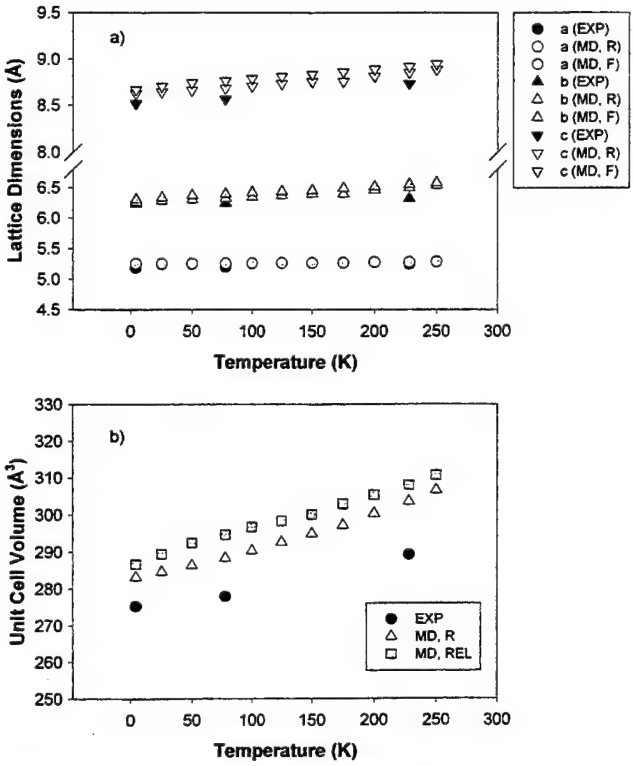

Figure 2. Variation of the lattice dimensions (a) and unit cell volume (b) with temperature from NPT-MD simulations using the rigid-body approximation (MD, R) and the flexible model (MD, F). The available experimental data from ref 7 (EXP) are also indicated.

atoms due to the rotational motion of the methyl group about the C−N bond would occur in the **b**−**c** plane only. Thus, the increasingly large librational motion occurring with increases in temperature would affect only the cell dimensions associated with the **b** and **c** axes. In the actual crystal, the arrangement of the molecules in the unit cell is such that the C−N bonds of all four are nearly perpendicular to the **c** axis (as can be seen in Figure 1). The angles that each C−N bond makes with the axes of the crystal cell are 40, 51, and 86° for the **a**, **b**, and **c** axes, respectively. This alignment of the molecules relative to these axes indicates that rotations of the methyl group about the C−N bond would more strongly affect the **b** and **c** axes. Indeed, by comparing the data in Figure 2a, it is clear that the major differences between NPT-MD data from the rigid and flexible

TABLE 5: Comparison of the Average Orientational Parameters (fractional coordinates sx, sy, sz and Euler angles Θ, Φ, Ψ) for the Four Molecules in the Unit Cell and of the Internal Geometrical Parameters of Nitromethane Molecule as Obtained from Trajectory Calculations at Different Temperatures; Corresponding Experimental Values (where available) Are Also Indicated[a]

	temperature(K)							
parameter	4.2 expt[b,c]	4.2 NPT-MD	4.2 ideal	78 expt[b,c]	78 NPT-MD	78 ideal	150 NPT-MD	150 ideal
sx1	0.3493	0.3513		0.3475	0.3483		0.3484	
sy1	0.4196	0.4284		0.4188	0.4288		0.4290	
sz1	0.3750	0.3682		0.3803	0.3722		0.3740	
sx2	0.1507	0.1487	0.1487	0.1525	0.1509	0.1517	0.1512	0.1515
sy2	−0.4196	−0.4284	−0.4284	−0.4188	−0.4291	−0.4288	−0.4290	−0.4290
sz2	−0.1250	−0.1318	−0.1318	−0.1197	−0.1279	−0.1278	−0.1262	−0.1260
sx3	−0.3493	−0.3513	−0.3513	−0.3475	−0.3494	−0.3483	−0.3488	−0.3485
sy3	−0.0804	−0.0717	−0.0716	−0.0812	−0.0711	−0.0712	−0.0705	−0.0710
sz3	0.1250	0.1317	0.1318	0.1197	0.1277	0.1278	0.1260	0.1260
sx4	−0.1507	−0.1488	−0.1487	−0.1525	−0.1513	−0.1517	−0.1516	−0.1515
sy4	0.0804	0.0716	0.0716	0.0812	0.0708	0.0712	0.0703	0.0710
sz4	−0.3750	−0.3683	−0.3682	−0.3803	−0.3719	−0.3722	−0.3739	−0.3740
Θ1	90.8	94.4		96.6	92.9		92.2	
Φ1	53.5	51.9		51.6	53.2		53.7	
Ψ1	238.9	245.3		240.1	245.4		245.4	
Θ2	−90.8	−94.4	−94.4	−96.6	−92.9	−92.9	−92.4	−92.2
Φ2	53.5	52.0	51.9	51.6	53.1	53.2	53.7	53.7
Ψ2	238.9	245.3	245.3	240.1	245.5	245.4	245.4	245.4
Θ3	89.2	85.5	85.6	83.4	87.2	87.1	87.7	87.8
Φ3	−53.5	−52.0	−51.9	−51.6	−53.1	−53.2	−53.8	−53.7
Ψ3	58.9	65.3	65.3	60.1	65.4	65.4	65.4	65.4
Θ4	−89.2	−85.6	−85.6	−83.4	−87.1	−87.1	−87.7	−87.8
Φ4	−53.5	−52.0	−51.9	−51.6	−53.2	−53.2	−53.7	−53.7
Ψ4	58.9	65.3	65.3	60.1	65.4	65.4	65.4	65.4

	temperature(K)				
parameter	4.2 expt[b]	4.2 NPT-MD	78 expt.[b]	78 NPT-MD	150 NPT-MD
C−N	1.481	1.497	1.488	1.499	1.499
C−H	1.098	1.088	1.077	1.089	1.090
$N-O_3$	1.209	1.230	1.198	1.230	1.231
$N-O_4$	1.223	1.229	1.226	1.230	1.231
HCH	111.6	110.7	111.2	110.6	110.5
HCN	107.3	108.2	107.7	108.2	108.2
CNO_3	118.9	118.1	119.1	117.8	117.8
CNO_4	117.8	117.7	116.8	117.8	117.9
O_3NO_4	123.3	124.3	124.1	124.2	124.2

[a] In the case of molecules 2−4 the ideal orientational parameters obtained based on $P2_12_12_1$ space group symmetry operators and the orientation parameters of molecule 1, positioned in the asymmetric unit, are given. [b] Experimental values from ref 7. [c] Unit cell fractional values have been shifted to fall within the range from −1/2 to 1/2.

potential models are in the expansions along the **b** and **c** axes while the variations for the case of the **a** axis are practically absent. The additional expansion due to the methyl group rotation can be also seen in Figure 2b where the volume values obtained using the flexible model are consistently larger than the corresponding data obtained for the rigid model.

In Table 5 we compare first the results of the average fractional coordinates and orientational Euler parameters of the four molecules in the unit cell with the corresponding experimental data (where available). These values are averaged over time and all unit cells in the simulation box. Additionally, in the same table we provide the "ideal" orientational Euler parameters for three of the four molecules of the unit cell relative to the orientation of the reference molecule in the asymmetric unit cell. These parameters have been calculated assuming the symmetry operations of the $P2_12_12_1$ space group. In this way we can analyze the degree of deviation of the predicted crystal structure from the $P2_12_12_1$ symmetry.

It is evident that increasing the temperature from 4.2 to 150 K does not produce any significant displacement of the molecular centers of mass and that the degree of rotational disorder is small. The largest deviations of the system from the orientational parameters corresponding to a perfect crystal with $P2_12_12_1$ symmetry are 0.0011 and 0.2° for the fractional coordinates and Euler angles, respectively. A similar conclusion is obtained for temperatures between 150 and 250 K (not shown). At $T = 4.2$ K, the largest deviation between the experimental and predicted molecular orientations is about 6.4° for the Euler angle Ψ (see Table 5), in agreement with previous MP findings. At $T = 78$ K this maximum deviation decreases to about 5.4°.

Additional support for the small degree of translation of the molecules inside the unit cell with the temperature increase can be obtained from the C···C RDFs given in Figure 3a. As can be seen, the RDFs at these temperatures correspond to well-ordered structures with correlation at long distances. The positions of the major peaks do not change significantly and the main temperature effect is the broadening of the peaks with partial overlapping of some of them.

The good agreement of the structural molecular parameters predicted by the model with experiment can be also observed by analyzing the internal coordinates (bond lengths and angles) indicated in Table 5. At 4.2 K the maximum deviations for bond lengths is about 1.7% and about 1.0% for bond angles. This

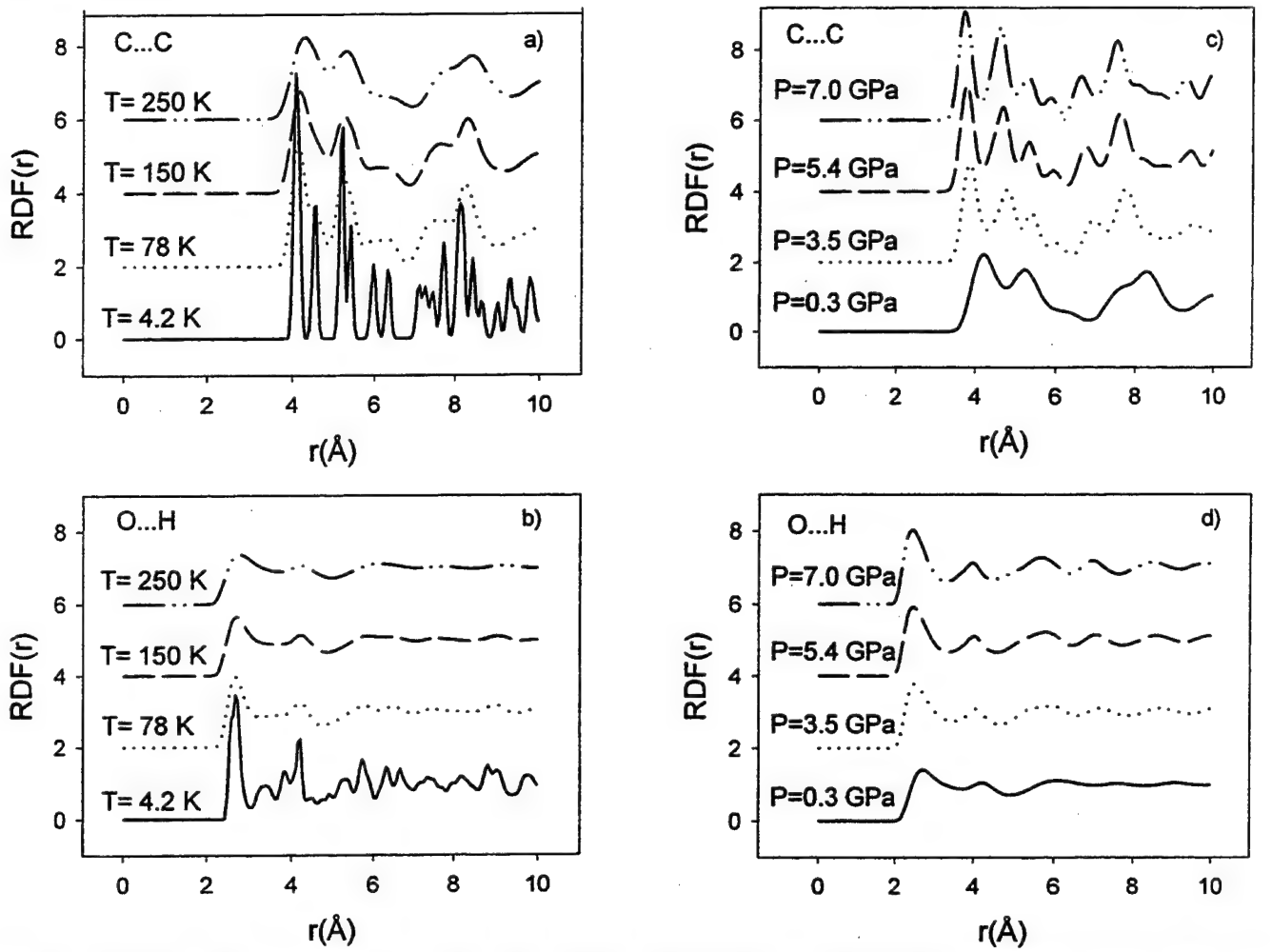

Figure 3. Radial distribution functions for C···C and O···H as functions of temperature (a−b) at atmospheric pressure and as function of pressure (c−d) at $T = 293$ K.

level of agreement is particularly good taking into account that in our potential parametrization, we have considered the internal geometrical parameters of the nitromethane molecule determined from gas-phase ab initio calculated values rather than parameters corresponding to nitromethane in the crystalline phase. These results suggest also a small influence of the lattice field on the internal parameters of the nitromethane molecule. Changes in predicted molecular structural parameters with temperature are negligible, again in agreement with experiment. The most significant change appears due to the internal rotation of the methyl group as a function of temperature. This is evident by inspecting the behavior of the radial distribution functions (RDFs) for the O···H intermolecular bonds given in Figure 3b. There is a rapid destruction of the correlation at long distances with the increase of temperature and consequently the individuality of the H atoms in the C−H···O bonds is lost. These effects can be understood as being due to the increase in rotational disorder of the methyl group with the increase of temperature.

The increase in the librational motion of the methyl group with temperature is illustrated in Figure 4. This figure shows the cumulative distributions of the $H_i-C_1-N_2-O_3$ ($i = 5-7$) dihedral angles at temperatures ranging from 4.2 to 150 K. These distributions have been determined from the molecular configurations recorded at every tenth step during trajectories of 16000 steps (12 ps). In this figure, the distributions are peaked at the angles corresponding to the equilibrium orientation of the methyl group in the low-temperature structure, namely, −78°, 42°, and 161° respectively. These angles are within 10° from those corresponding to the experimental structure determined by the neutron diffraction technique.[7] As can be seen in Figure 4 the increase of temperature does not change the position of these peaks. However, the distributions broaden with temperature, indicating an increase in librational motion with temperature. For the case of the potential model with the increased HCNO torsional barrier (M2) we have found that the agreement between the predicted (−85°, 34°, 154°) and experimental (−88°, 31°, 151°) torsional angles is even better, with deviations within 3°. Similarly, in this case the increase of temperature did not modify the position of the peaks in the cumulative distributions.

The magnitudes of the methyl group libration have been previously determined experimentally for deuterated nitromethane in the temperature range 4.2−125 K using neutron diffraction powder experiments.[7] As can be seen in Figure 5 where the experimental values are compared with our results the agreement is quite good for the entire temperature range 25−125 K. For example, the experimental results indicate that at 25 and 125 K the rms amplitudes of libration of the CD_3 group are ~13° and 25°, respectively. Our NPT-MD calculations of deuterated nitromethane predict rms amplitudes of libration of 12° at 25 K and 23° at 125 K (see Figure 5). Comparison of the amplitude of libration at 4.2 K with experiment is not appropriate, since quantum mechanical effects would be significant at this temperature. The experiments[7] suggest that the amplitude of libration at this temperature is as large as that at

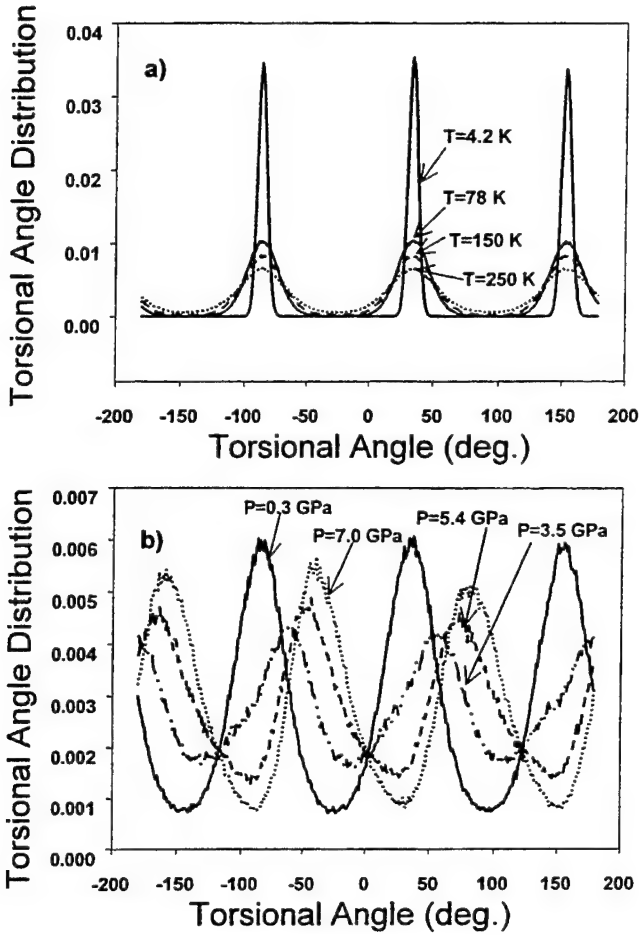

Figure 4. Distribution of the $H_i-C_1-N_2-O_3$ (i = 5,6,7) dihedral angles for all nitromethane molecules in the simulation box as a function of temperature (a) and pressure (b).

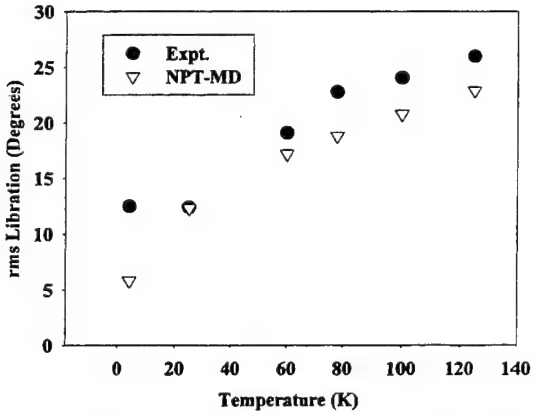

Figure 5. Root-mean-square amplitude of libration of the methyl group in CD_3NO_2 as a function of temperature.

25 K; our classical simulations predict a value that is smaller by ~7°. Previous quasielastic and inelastic neutron scattering studies[8] performed on protonated nitromethane have provided additional information about the temperature dependence of the rotational reorientation of the methyl groups. By assuming a 3-folded reorientation model and an Arrhenius dependence ($\sim e^{Ea/kT}$) of the mean residence times of methyl groups on the temperature T, an activation barrier of 234 cal/mol to the methyl group rotation has been determined. However, more recent experimental studies based on infrared and Raman measurements have indicated higher activation energies with values of 401 cal/mol[16] and 576 cal/mol,[10] respectively. We monitored

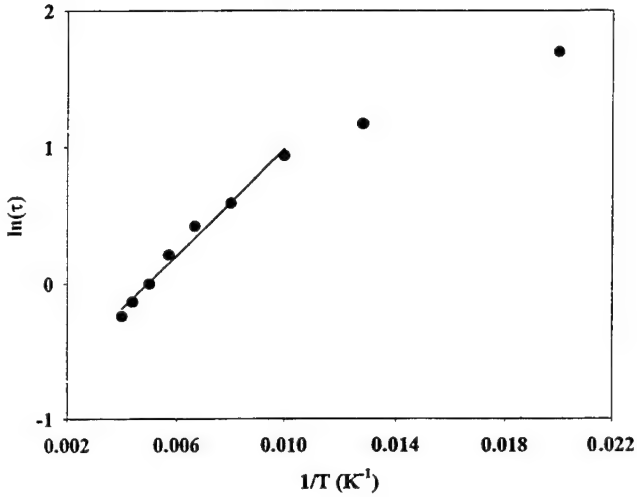

Figure 6. The mean residence times τ of the methyl group versus inverse temperature. The activation energy of 387 cal/mol is obtained from the slope of the least-squares linear fit to the data in the region of higher temperatures (125−250 K) indicated by a solid line.

the frequency of 120° methyl group rotations for the duration of 12 ps in trajectories integrated at temperatures ranging from 4.2 to 250 K. From these trajectories we have observed that methyl groups undergo large vibrational amplitudes, indicative of small barrier heights for torsional motions in agreement with experimental findings.

To obtain a more quantitative description of the internal rotational motion we have considered the evaluation of temperature effects on the rates of reorientation of the methyl group. A "rotational jump" was defined in the following manner. At the beginning of each trajectory, the $H_i-C_1-N_2-O_3$ angles (i = 5−7) of each molecule were calculated. Each angle was assigned to one of the three minima in the 3-fold rotational potential by virtue of its proximity to the minima, and the time denoted as t_0. The minima corresponded to the values of the $H_i-C_1-N_2-O_3$ angles (i = 5−7) in the low-temperature structure, i.e., −78°, 42°, and 161°, respectively. The assignment of these angles to the minima are made at each subsequent step in the trajectory and compared to the original assignment at t_0. When the assignments for all three of the $H_i-C_1-N_2-O_3$ angles differ from the original assignments at t_0, it is assumed that a rotational jump has occurred. At this point, the time interval between the time of the new assignments and t_0 was recorded. The value of t_0 was reset to the time of the new assignments, and the process repeated for the duration of the trajectory. Methyl group reorientation rates at each temperature were determined by extracting first-order rate coefficients from linear fits of plots of ln(P) versus time, where P is the fraction of nitromethane molecules that have not jumped at time t. The lifetimes indicate first-order behavior. An Arrhenius plot of the residence times, which are the inverse of the reorientation rates, is shown in Figure 6. Fitting a line to all the points in Figure 6 predicts E_a = 241 cal/mol. However, the nonlinearity of the Arrhenius plot is a result of the statistical errors in the low-temperature rates, and if we base our prediction on the 7 points for the highest temperaures (100−250 K) we predict E_a = 387 cal/mol. These values are in accord with the reported experimental activation energies (234−576 cal/mol).[8,10,16]

B2. Pressure Effects. The calculated lattice dimensions at different pressures are given in Table 6 and a visual comparison with the experimental data is presented in Figure 7. For the entire pressure range investigated (0.3−7 GPa) the differences between the calculated NPT-MD data using the flexible potential

TABLE 6: Lattice Parameters Obtained in Crystal Packing and NPT-MD Calculations for Nitromethane as a Function of Pressure

	NPT-MD				molecular packing			
	lattice lengths (Å)			unit cell	lattice lengths (Å)			unit cell
press (GPa)	*a*	*b*	*c*	volume (Å^3)	*a*	*b*	*c*	volume (Å^3)
0.30	5.2070	6.4829	8.8597	299.0666	5.2068	6.1989	8.5628	276.3758
0.33	5.2006	6.4874	8.8416	298.2833	5.2040	6.1929	8.5576	275.7927
0.50	5.1713	6.4236	8.7800	291.6500	5.1861	6.1561	8.5172	271.7649
1.00	5.0997	6.3001	8.6595	278.2166	5.1397	6.0786	8.4295	262.9498
2.00	4.9827	6.1706	8.4936	261.1500	5.0656	5.9716	8.3055	250.5347
3.00	4.8963	6.0797	8.3826	249.5166	5.0051	5.8988	8.2150	241.6301
3.50	4.8603	6.0448	8.3392	245.0000	4.9792	5.8684	8.1772	237.9397
4.00	4.8245	6.0139	8.2955	240.6833	4.9536	5.8447	8.1421	234.6472
5.00	4.7652	5.9600	8.2265	233.6500	4.9054	5.8085	8.0780	228.8875
5.45	4.7426	5.9412	8.2001	231.0500	4.8843	5.7969	8.0517	226.5996
6.00	4.7116	5.9145	8.1666	227.5833	4.8527	5.7982	8.0161	223.9448
6.50	4.6898	5.8925	8.1404	224.9666	4.7698	5.9135	7.9484	221.2719
7.00	4.6666	5.8733	8.1162	222.4500	4.7171	5.9801	7.8992	218.8226

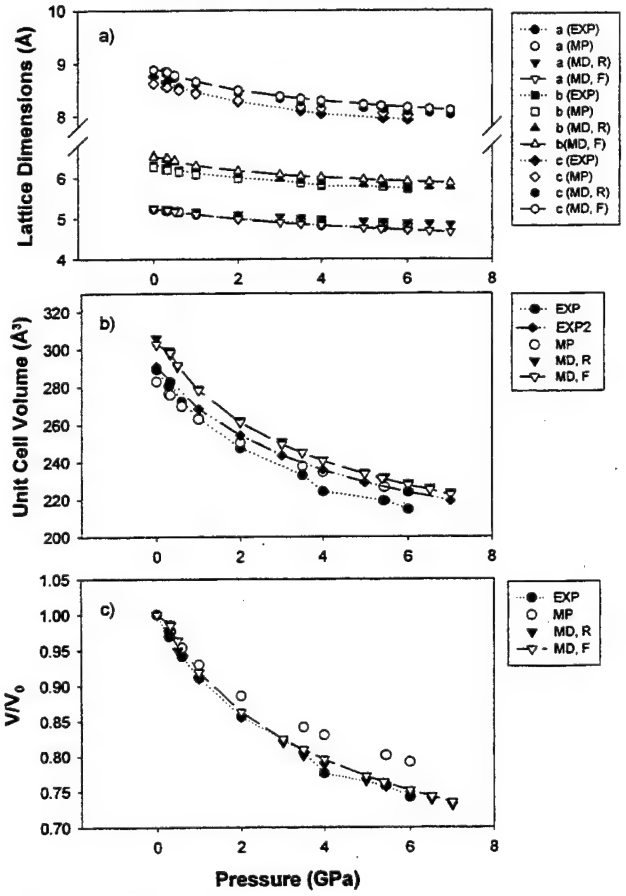

Figure 7. Pressure variation of the lattice dimensions (a), unit cell volume (b), and volume compression V/V_0 on the external pressure. The calculated data from molecular packing (MP), NPT-MD simulations using the rigid-body approximation (MD,R) and the flexible model (MD,F) are represented. The corresponding experimental data from refs 9 (EXP) and 12 (EXP2), respectively, are also indicated.

and the experimental crystallographic parameters are small. By considering as reference the experimental data determined by Cromer et al.[9] we find that in the low-pressure region (0.3 GPa) the percentage errors for lattice dimensions **a**, **b**, and **c** are 0.3%, 3.4%, and 2.9%, respectively. A similar good correspondence is found in the high-pressure region (6.0 GPa) where the percentage errors are 0.4%, 3.5%, and 2.4% for the **a**, **b**, and **c** lattice dimensions, respectively. Moreover, for the entire pressure range investigated the NPT-MD predicted volume compression closely follows the corresponding variation observed experimentally (see Figure 7b). In Figure 7b we have also represented the experimental values reported by Yarger and Olinger.[12] As can be seen in this case the agreement with our calculated unit cell volumes is even better than that found with data provided by Cromer et al.,[9] with decreasing deviations from about 3.6% at 1 GPa to 1.4% at 7 GPa.

The MP results obtained using the rigid body approximation generally follow the predictions obtained using the flexible potentials, particularly in the low-pressure region. Also, the agreement between the NPT-MD data obtained using the rigid molecular assumption is surprisingly good with NPT-MD data using the flexible model. This fact indicates that for the pressure region investigated, the compression of the lattice is almost entirely due to a reduction of intermolecular distances. These effects can be also seen from the inspection of the normalized dependence of the unit cell volume on pressure given in Figure 7c. In this plot the experimental curve[9] and those predicted by the flexible and rigid models are practically superimposed for the entire range of pressures investigated. The values obtained in the MP calculations start to deviate more significantly from the experimental results, particularly for pressures above 5 GPa. These facts indicate that the lattice compressibility becomes less well represented in these calculations as the pressure is increased. However, the present set of results support our previous findings[6] that in the region of low to moderate pressures (~5 GPa) the MP calculations can be used as an alternative tool to describe the changes of the unit cell geometrical parameters but at a fraction of the computational cost involved in MD simulations.

Further comparison of the predicted and experimental lattice parameters can be obtained by extrapolating to zero pressure and 293 K the results of different studies, which in principle should coincide. As in previous experimental studies,[7,9,12] the extrapolation is taken because at room temperature nitromethane is in the liquid phase. The coefficients of cubic fits in pressure of the predicted lattice parameters and unit cell volume to the data predicted by our flexible potential are given in Table 7. In Table 8 we compare the zero-pressure extrapolated data obtained in this work to those of previous experimental investigations. Particularly, we have considered both the low-temperature data obtained by Trevino et al.[7] and extrapolated to room temperature as well as the high-pressure values determined previously[9,12] and extrapolated to zero pressure. As can be seen in Table 8, our crystal lattice dimensions are within 2.2%, 2.9%, and 3.4% from the data given in refs 7, 9, and, 12, respectively. This level of agreement is satisfactory taking into account the relative large deviations between different sets of experimental values.

TABLE 7: Coefficients of the Cubic Fit in Pressure (GPa) of the Lattice Constants and Unit Cell Volume

	α_0	α_1	α_2	α_3
a(Å)	5.246 Å	-1.601×10^{-1} Å GPa^{-1}	1.704×10^{-2} Å GPa^{-2}	-0.858×10^{-3} Å GPa^{-3}
b(Å)	6.537 Å	-2.475×10^{-1} Å GPa^{-1}	3.836×10^{-2} Å GPa^{-2}	-2.379×10^{-3} Å GPa^{-3}
c(Å)	8.911 Å	-2.711×10^{-1} Å GPa^{-1}	3.788×10^{-2} Å GPa^{-2}	-2.210×10^{-3} Å GPa^{-3}
V(Å^3)	305.17 Å	$-2.885 \times 10^{+1}$ Å^3 GPa^{-1}	4.123 Å^3 GPa^{-2}	-2.428×10^{-1} Å^3 GPa^{-3}

TABLE 8: Comparison of the Lattice Constants for Solid Nitromethane Extrapolated to 293 K and 0 GPa and of the Murnagham Equation Coefficients (eq 8) from Present Calculations and Various Studies

parameter	ref 7 (low temperature)	ref 9 (high pressure)	ref 10 (high pressure)	present work
a_0(Å)	5.270	5.227	5.197	5.238
b_0(Å)	6.375	6.330	6.292	6.514
c_0(Å)	8.832	8.758	8.747	8.889
V_0(Å^3)	296.72	289.77	286.02	302.80
V_{0fit}(Å^3)		292.7	291.87	310.35
B_0(GPa)		7.0	9.14	6.78
B_0'		5.7	6.04	5.88

Another set of parameters we have used to assess the accuracy of our potential is represented by the coefficients of the Murnaghan equation:[9,35]

$$P(V) = \frac{B_0}{B_0'}\left[\left(\frac{V_0}{V}\right)^{B_0'} - 1\right] \quad (8)$$

which has been used to fit the dependence of the unit cell volume on pressure. In eq 8, V is the volume at pressure P, V_0 is the volume at $P = 0$ (and allowed to be varied in the fitting procedure), B_0 is the bulk modulus at zero pressure, and $B_0' = dB_0/dP$. In Table 8 we present the best-fit parameters obtained from our NPT-MD calculated values together with the corresponding experimental data. Our results clearly support the experimental findings obtained by Cromer et al.[9] with relative percentage deviations of 3.2% and 3.1% for the bulk modulus and its pressure derivative values, respectively.

From the compression data for our lattice parameters we have also determined the variation of cell edge moduli, $-X\,\partial P/\partial X$, as a function of pressure (see Figure 8). Our results indicate that the compressibilities of the **b** and **c** axes are close to each other, the **c** axis being the least compressible at high pressures. These findings are similar to those obtained by Cromer et al.[9] and represented for comparison in Figure 8. However, the differences in compressibilities for the **b** and **c** axes with pressure are more pronounced in the experimental case than our data show. Additionally, we find that the **a** axis is the least compressible at low pressures but becomes the most compressible for pressures above 2 GPa. This trend is also present in the Cromer et al. data[9] and has been also noted previously by Yarger and Olinger.[12] These authors[12] have suggested that the behavior of the compressive response of the unit cell, particularly with regard to the **a** axis, could be explained by the formation of "chains" of molecules, linked by bonds between the nitro and methyl groups of the neighboring molecules as they are compressed. Unfortunately, there is no additional theoretical or experimental support to identify such a mechanism and further studies, particularly based on ab initio calculations, are necessary to explore the formation of such chainlike structures. The only available data are related to a density functional theoretical study performed at the B3LYP/6-31G** level to describe the interaction between two nitromethane molecules separated by distances ranging from 1.6 to 3.5 Å.[36] The molecules were initially arranged with the methyl group on one molecule facing the nitro group on the second (an arrangement that would correspond to compression along the **a** axis). As the molecules were brought closer together, the potential energy first showed a steep increase, and the methyl group was "flattened" to the point that the hydrogen and carbon atoms were located in the same plane. Further decreases in the intermolecular distance led to reaction to form products HONO, CH_2O, and CH_3O. Thus, these calculations do not support the hypothesis that "chains" of molecules are formed through new bonding of intermolecular methyl−nitro group interactions upon compression of the **a** axis. However, more detailed analyses corresponding to the specific interactions that take place in crystals are necessary. The change in the ordering of the most compressible axes appears to occur near the pressure at which the equilibrium orientation of the methyl group has changed to 45° relative to the crystal at low pressure.[9] This pressure-induced rotational reorientation provides another test of our interaction potential, the results of which we discuss next.

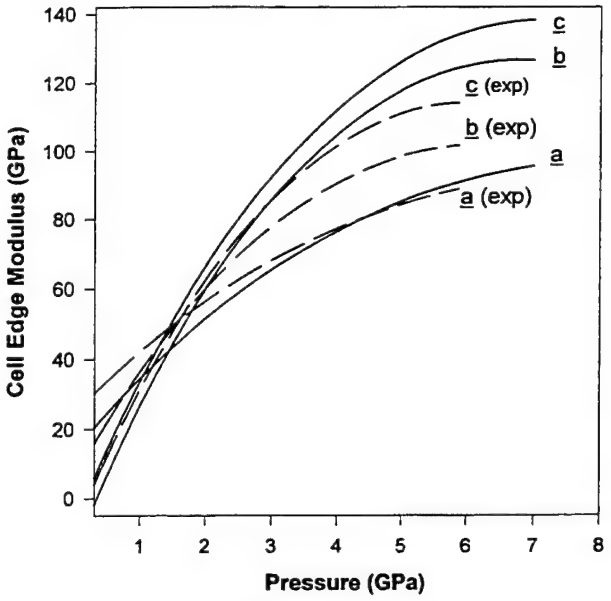

Figure 8. The variation of the cell edge moduli as a function of pressure from the present calculation and from experimental data given in ref 9.

Changes in the rotational motion of the methyl group as a function of pressure can be observed through RDFs for the O···H intermolecular bonds. We have already seen from previous sections that RDFs for O···H intermolecular bonds indicate an increase of the degree of rotational disorder of the methyl group as the temperature increases (at ambient pressure). The RDFs for O···H intermolecular bonds follow a reverse trend when the pressure is increased (at ambient temperature), as shown in Figure 3d. In this case the spectrum becomes better resolved with pressure increases, indicating a significant decrease of the amplitude of methyl rotations around the equilibrium positions.

An illustration of the dynamic behavior of the methyl group librations with increasing pressure is presented in Figure 9. In this figure, the time histories of the $H_i-C_1-N_2-O_3$ ($i = 5-7$) torsional angles of one of the molecules in the crystal at two

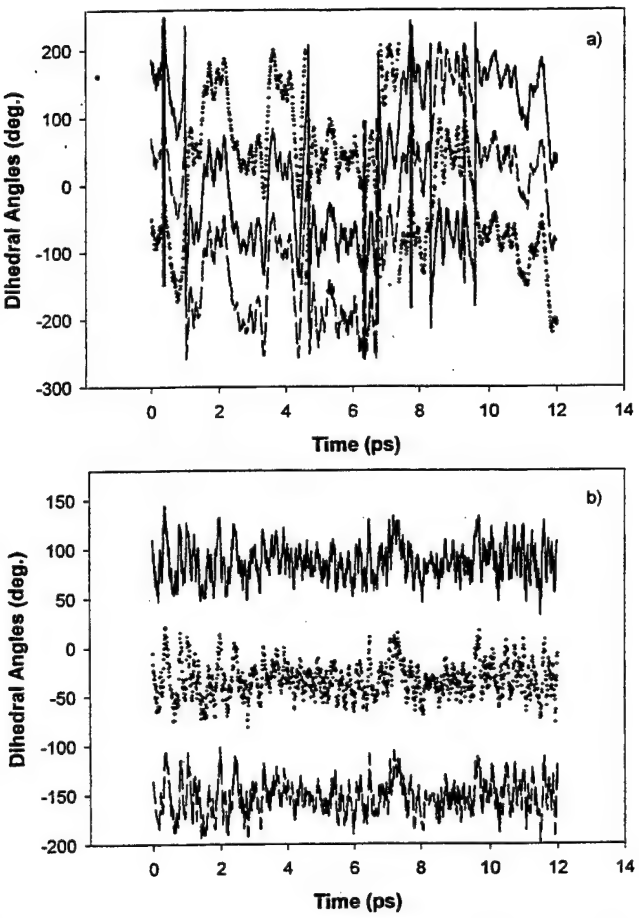

Figure 9. The time history of the variation of $H_i-C_1-N_2-O_3$ (i = 5,6,7) dihedral angles for one of the nitromethane molecules from trajectories performed at P = 0.3 GPa (a), and P = 7.0 GPa (b), and T = 293 K. For visualization purposes some of the angles have been shifted by ±360°.

different pressures (T = 293 K) are represented. In the low-pressure case, the methyl group rotation is slightly hindered, as methyl group "jumps" from one equilibrium configuration to another are seen at times 0.5 and 5 ps in the time histories. In the high-pressure regime the torsional angles oscillate around well-defined equilibrium values and the jumps between the equilibrium wells are absent. Also, the equilibrium configuration for the methyl group changes with pressure, as illustrated by the time histories in Figure 9. To determine these equilibrium values we have analyzed the cumulative distributions of the $H_i-C_1-N_2-O_3$ (i = 5−7) torsional angles for all the molecules in the simulation box during trajectories executed at different pressures, T = 293 K. The corresponding data obtained in these analyses are represented in Figure 4b. When compared to the distributions of these angles as a function of temperature (see Figure 4a), the increase of pressure has a totally different effect on the distribution of torsional angles. In this case there is a continuous shift of the peak positions with pressure such that between 0.3 and 5.4 GPa this shift amounts to about 41° while between 0.3 GPa and 7.0 GP the corresponding variation is about 50°. These data agree very well with the experimental findings obtained by Cromer et al.[9] in which the methyl group was found to be rotated by about 45° relative to the low-temperature configuration.

We next explore the basis for the rotational reorientation with pressure by comparing properties of two crystals, one in which the methyl groups are rotated and one in which the methyl groups are in the arrangement corresponding to the low-temperature, low-pressure configuration. Both crystals have $P2_12_12_1$ symmetry and use the structural parameters corresponding to averages obtained in our simulations. The only difference between the two models is in the arrangement of the hydrogens of the methyl group. In one model, the methyl group is rotated by 50° relative to the low-temperature, low-pressure crystal. In the second model, the methyl group is in the same arrangement as the low-temperature, low-pressure crystal. We first compared the total potential energy for the two systems using structural parameters for T = 4.2 K at 0 atm pressure. The model in which the methyl group is not rotated has a total potential energy that is lower by 3.5 kJ/mol per molecule. In that model, the repulsive N−H contributions to the total potential are greater (by 4.9 kJ/mol), but the repulsive H−H interactions are lower by 1.4 kJ/mol. The attractive C−H contribution is larger for the model in which the methyl group is rotated by 0.9 kJ/mol. The largest difference in contribution to the total potential is due to the O−H contributions, which are more attractive by 6.1 kJ/mol for the low-energy crystal. These combined effects account for the difference in energy between the two models.

For model crystals using structural parameters corresponding to a pressure of 7 GPa and temperature of 293 K, the model in which the methyl groups are rotated by 50° has a total potential energy that is lower by 35 kJ/mol per molecule than the model in which the methyl groups are not rotated. The energy difference (per molecule) is due mainly to the H−N, O−H, and H−H interactions. For the model in which the methyl group is rotated by 50°, there is a net decrease of 17.0 kJ/mol for the N−H repulsive interactions, a net increase of 1.1 kJ/mol for the C−H attractive interactions, and a net increase of 26.8 kJ/mol for the O−H attractive interactions. H−H repulsions are greater in the rotated crystal model by 10 kJ/mol. For both pressures, the largest differences in the total potential energy are due to the contributions of O−H and N−H interactions. The results indicate that the methyl group rotation with pressure allows for the enhancement of the O−H attractions while reducing the N−H repulsions.

Structural molecular parameters predicted by the model and experimental values (where available) as a function of pressure are given Table 9. The most significant changes in molecular structure with pressure are the compression of the C−N bond and the distortion of the $C_1-N_2-O_4$ angle. These trends were also seen in experiment; however, the effects were more pronounced. In the experimental results, the C−N bond is compressed by 0.08 Å at 3.5 GPa, and the heavy atom angles have changed by ~4°. In our model, the corresponding C−N bond compression is only 0.01 Å, and the heavy atom angles have not significantly changed.

A comparison of the average fractional coordinates and orientational Euler parameters for the four molecules in the unit cell is given in Table 9. All orientational parameters of the four molecules in the unit cell were averaged over time and all unit cells in the simulation space. We have also generated orientational parameters for the four molecules in the unit cell assuming perfect $P2_12_12_1$ symmetry in the manner described earlier. The only complete set of fractional coordinates for all atoms in the Cromer et al.[9] study corresponded to 3.5 GPa, 293 K, with the assumption that the C−H bonds and H−H distances are 1.0 and 1.63 Å, respectively. The simulation results are in good agreement with these experimental data, indicating that the model reasonably represents the crystal under moderate pressure. Comparison of the averages of the four molecules in the unit cell with those with $P2_12_12_1$ symmetry indicate that the space

TABLE 9: Comparison of the Average Orientational Parameters (fractional coordinates sx, sy, sz and Euler angles Θ, Φ, Ψ) for the Four Molecules in the Unit Cell and of the Internal Geometrical Parameters of Nitromethane Molecule as Obtained from Trajectory Calculations at Different Pressures; Corresponding Experimental Values (where available) Are Also Indicated[a]

	pressure(GPa)						
parameter	0.3 NPT-MD	0.3 ideal	3.5 expt[b,c]	3.5 NPT-MD	3.5 ideal	7.0 NPT-MD	7.0 ideal
sx1	0.3488		0.3453	0.3391		0.3316	
sy1	0.4284		0.4055	0.4311		0.4304	
sz1	0.3765		0.3844	0.3855		0.3938	
sx2	0.1519	0.1512	0.1547	0.1609	0.1609	0.1684	0.1684
sy2	−0.4243	−0.4284	−0.4055	−0.4300	−0.4311	−0.4295	−0.4304
sz2	−0.1235	−0.1235	−0.1156	−0.1139	−0.1145	−0.1059	−0.1062
sx3	−0.3479	−0.3488	−0.3453	−0.3388	−0.3391	−0.3314	−0.3316
sy3	−0.0687	−0.0716	−0.0945	−0.0688	−0.0689	−0.0693	−0.0696
sz3	0.1233	0.1235	0.1156	0.1149	0.1145	0.1060	0.1062
sx4	−0.1525	−0.1512	−0.1547	−0.1614	−0.1609	−0.1685	−0.1684
sy4	0.0686	0.0716	0.0945	0.0700	0.0689	0.0706	0.0696
sz4	−0.3769	−0.3765	−0.3844	−0.3853	−0.3855	−0.3940	−0.3938
Θ1	91.4		91.3	90.6		89.5	
Φ1	54.7		55.8	56.2		57.0	
Ψ1	245.3		242.9	248.0		249.3	
Θ2	−91.4	−91.4	−91.3	−89.9	−90.6	−89.1	−89.5
Φ2	54.7	54.7	55.8	56.3	56.2	57.0	57.0
Ψ2	245.3	245.3	242.9	247.7	248.0	249.0	249.3
Θ3	88.4	88.6	88.7	89.6	89.4	90.7	90.5
Φ3	−54.8	−54.7	−55.8	−56.3	−56.2	−57.1	−57.0
Ψ3	65.2	65.3	62.9	67.8	68.0	69.0	69.3
Θ4	−88.6	−88.6	−88.7	−89.9	−89.4	−90.7	−90.5
Φ4	−54.6	−54.7	−55.8	−56.2	−56.2	−57.0	−57.0
Ψ4	65.2	65.3	62.9	67.7	68.0	69.0	69.3

	pressure(GPa)				
parameter	0.3 expt[b]	0.3 NPT-MD	3.5 expt[b]	3.5 NPT-MD	7.0 NPT-MD
C−N	1.55	1.500	1.47	1.489	1.481
C−H		1.092		1.088	1.084
$N-O_3$	1.21	1.231	1.21	1.228	1.224
$N-O_4$	1.20	1.231	1.26	1.228	1.226
HCH		110.5	110.7	110.6	110.8
HCN		108.1	107.9	107.9	107.7
CNO_3	117.7	117.7	118.4	117.0	115.9
CNO_4	116.2	117.9	119.9	118.8	119.9
O_3NO_4	125.9	124.1	121.6	123.9	123.9

[a] In the case of molecules 2−4, the ideal orientational parameters obtained based on $P2_12_12_1$ space group symmetry operators and the orientation parameters of molecule 1, positioned in the asymmetric unit, are also indicated. [b] Experimental values from ref 9. Since the hydrogen atom positions could not be resolved at 0.3 GPa, the orientational parameters for nitromethane at this pressure are not available for comparison. [c] Unit cell fractional values have been shifted to fall within the range from −1/2 to 1/2.

group symmetry is conserved with pressure, as observed in experiment.[9]

Also, as opposed to the temperature effects, which tend to increase the degree of disorder in system, the increase of pressure has the opposite effect. As can be seen in Figure 3c the peaks of RDFs for C···C intermolecular distances shift toward smaller distance values with increasing pressure, indicating the compression of the material. Moreover, more and more peaks regain their individuality with pressure increases, indicating an increase in the degree of rotational and translational order.

V. Conclusions

We have developed a classical potential for simulation of solid nitromethane containing both intra- and intermolecular potential terms. The parametrization of the intramolecular potential has been done on the basis of the results of ab initio calculations performed on the isolated nitromethane molecule at the B3LYP/6-31G* level. Both structural geometrical parameters as well as data about the vibrational frequencies and their eigenvectors have been used in the fitting procedure. The intermolecular potential used in these calculations is of the Buckingham 6-exp form and was previously developed for RDX crystals[1] and showed to be transferable to 30 nitramine crystals[4] and to 51 other non-nitramine crystals.[5]

Molecular packing calculations using the proposed set of intermolecular parameters and the set of HF charges indicate an accurate prediction of crystallographic parameters with deviations less than 1.21% for the lattice edges. Additionally, the predicted lattice energy of nitromethane is in acceptable agreement with previous theoretical estimations.[34]

The tests of this potential in NPT-MD simulations indicate that the prediction of the crystallographic parameters is also well reproduced as a function of temperature with deviations between 1.7 and 3.6% from the experimental data[7,9] for the temperature range 4.2−228 K. Moreover, the present potential is able to predict changes of the crystallographic parameters with pressure similar to those observed experimentally.[9] A similar good agreement is found for the bulk modulus and its pressure derivative. At zero pressure the predicted bulk modulus is $B_0 = 6.78$ GPa while the corresponding experimental value is 7.0 GPa.[9]

The results of MD and NPT-MD simulations performed using the rigid-body approximation indicate that the predicted values in these cases are similar to those obtained from the flexible model particularly for pressures up to about 5 GPa.

Both RDFs as well as the analyses of the HCNO dihedral angle distributions during trajectories calculations obtained using the flexible model indicate two distinctive regimes for methyl group rotational dynamics. There is an increase of the degree of rotation of the methyl group with temperature increase (at ambient pressure) without significant changes of the average equilibrium positions. On the other hand, at ambient temperature, the increase of pressure causes a continuous shift of the average equilibrium positions of the H atoms relative to the $C-NO_2$ plane. A comparison of the contributions of the individual intermolecular interactions to the total potential energies for crystals in which the methyl groups are in the low-temperature, low-pressure configuration or arranged in the high-pressure configuration show that at high pressures, the O−H attractive interactions are enhanced upon methyl group rotation in the crystal while the N−H repulsive interactions are decreased; the remaining intermolecular interactions do not change significantly between the two models.

The success of the present potential model to describe the prototypical explosive, nitromethane, conjugated with the performances of the present intermolecular potential to describe a large number of important energetic materials, provides further incentives to develop these models and to extend their applications to more subtle effects such as the energy transfer[37,38] and reactions in condensed phases.

Acknowledgment. We are pleased to acknowledge many inspiring and helpful discussions with Dr. S. F. Trevino. This work was supported by the Strategic Environmental Research and Development Program (SERDP). D.L.T. gratefully acknowledges support by the U.S. Army Research Office under Grant DAAG55-98-1-0089.

References and Notes

(1) Sorescu, D. C.; Rice, B. M.; Thompson, D. L. *J. Phys. Chem.* **1997**, *B101*, 798.

(2) Sorescu, D. C.; Rice, B. M.; Thompson, D. L. *J. Phys. Chem.* **1998**, *B102*, 948.

(3) Sorescu, D. C.; Rice, B. M.; Thompson, D. L. *J. Phys. Chem.* **1998**, *B 102*, 6692.

(4) Sorescu, D. C.; Rice, B. M.; Thompson, D. L. *J. Phys. Chem.* **1998**, *A 102*, 8386.

(5) Sorescu, D. C.; Rice, B. M.; Thompson, D. L. *J. Phys. Chem.* **1999**, *A 103*, 989.

(6) Sorescu, D. C.; Rice, B. M.; Thompson, D. L. *J. Phys. Chem.* **1999**, *B 103*, 6783.

(7) Trevino, S. F.; Prince, E.; Hubbard, C. R. *J. Chem. Phys.* **1980**, *73*, 2996.

(8) Trevino, S. F.; Rymes, W. H. *J. Chem. Phys.* **1980**, *73*, 3001.

(9) Cromer, D. T.; Ryan, R. R.; Schiferl, D. *J. Phys. Chem.* **1985**, *89*, 2315.

(10) Grošev, V. M.; Stelzer, F.; Jocham, D. *J. Mol. Structure* **1999**, *476*, 181.

(11) Jones, W. M.; Giauque, W. F. *J. Am. Chem. Soc.* **1947**, *69*, 983.

(12) Yarger, F. L.; Olinger, B. *J. Chem. Phys.* **1986**, *85*, 1534.

(13) Piermarini, G. J.; Block, S.; Miller, P. *J. Phys. Chem.* **1989**, *93*, 457.

(14) Cavagnat, D.; Magerl, A.; Vettier, C.; Anderson, I. S.; Trevino, S. F. *Phys. Rev. Lett.* **1985**, *54*, 193.

(15) Tannebaum, E.; Myers, R. J; Gwinn, W. D. *J. Chem. Phys.* **1956**, *25*, 42.

(16) Remizov, A. B.; Musayakaeva, R. H. *Opt. Spektrosk.* **1975**, *38*, 226.

(17) Frisch, M. J.; Trucks, G. W.; Schlegel, H. B.; Gill, P. M. W. Johnson, B. G.; Robb. M. A.; Cheeseman, J. R.; Keith, T.; Patersson, G. A.; Montgomery, J. A.; Raghavachari, K.; Al-Laham, M. A.; Zakrzewski, V. G.; Ortiz, J. V.; Foresman, J. B.; Cioslowski, J.; Stefanov, B. B.; Nanyakkara, A.; Challacombe, M.; Peng, C. Y.; Ayala, P. Y.; Chen, W.; Wong, M. W.; Andres, J. L.; Replogle, E. S.; Gomperts, R.; Martin, R. L.; Fox, D. J.; Binkley, J. S.; Defrees, D. J.; Baker, J.; Stewart, J. P.; Head-Gordon, M.; Gonzales, C.; Pople, J. A. *Gaussian 94*, Revision C.3; Gaussian, Inc.: Pittsburgh, PA, 1995.

(18) Möller, C. M. S. *Phys. Rev.* **1934**, *46*, 618.

(19) Rice, B. M.; Thompson, D. L. *J. Chem. Phys.* **1990**, *93*, 7986.

(20) (a) Becke, A. D. *J. Chem. Phys.* **1993**, 98, 5648. (b) Lee, C.; Yang, W.; Parr, R. G. *Phys. Rev.* **1988**, *B41*, 785.

(21) Hehre, W.; Radom, L.; Schleyer, P. v. R.; Pople, J. A. *Ab Initio Molecular Orbital Theory*; Wiley-Interscience: New York, 1986.

(22) Rice, B. M.; Chabalowski, C. F.; Adams, G. F.; Mowrey, R. C.; Page, M. *Chem. Phys. Lett.* **1991**, *184*, 335.

(23) Forseman, J. B.; Frisch, A. In *Exploring Chemistry with Electronic Structure Methods*; Gaussian, Inc.: Pittsburgh, PA, 1996.

(24) (a) Wells, A. J.; Wilson, E. B. *J. Chem. Phys.* **1941**, *9*, 314. (b) Smith, D. C.; Pan, C.; Nielsen, J. R. *J. Chem. Phys.* **1950**, *18*, 706. (c) Jones, W. J.; Sheppard, N. *Proc. R. Soc. London Ser.* A **1968**, *304*, 135. (d) Trinquecoste, C.; Rey-Lafon, M.; Forel, M.-T. Spectrochim. Acta A **1974** *30*, 813. (e) McKean, D. C.; Watt, R. A. *J. Mol. Spectrosc.* **1976**, *61*, 184.

(25) Pertsin, A. J.; Kitaigorodsky, A. I. *The Atom-Atom Potential Method, Applications to Organic Molecular Solids*; Springer-Verlag: Berlin, 1987.

(26) Desiraju, G. R. *Crystal Engineering: The Design of Organic Solids*; Elsevier: Amsterdam, 1989.

(27) Gibson, K. D.; Scheraga, H. A. *J. Phys. Chem.* **1995**, *99*, 3752.

(28) Gibson, K. D.; Scheraga, H. A. *LMIN*: A Program for Crystal Packing, QCPE, No. 664.

(29) Melchionna, S.; Ciccotti, G.; Holian, B. L. *Mol. Physics* **1993**, *78*, 533.

(30) DL_POLY is a package of molecular simulation routines written by W. Smith and T. R. Forester, copyright The Council for the Central Laboratory of the Research Councils, Daresbury Laboratory at Daresbury, Nr. Warrington, 1996.

(31) Allen, M. P.; Tildesley, D. J. *Computer Simulation of Liquids*; Oxford University Press: New York, 1989.

(32) Fincham, D. *Molecular Simulation* **1992**, *8*, 165.

(33) *Fundamentals of Crystallography*; Giacovazzo, C., Ed.; Oxford University Press: New York, 1992.

(34) The enthalpy of sublimation for nitromethane has been communicated by P. Politzer and has been obtained based on the method described in Politzer, P.; Murray, J. S.; Grice, M. E.; DeSalvo, M.; Miller, E. M. *Mol. Phys.* **1997**, *92*, 923.

(35) Murnaghan, F. D. In *Finite Deformation of an Elastic Solid*; Dover Publications: New York, 1951; p 73.

(36) Cook, M. D.; Fellows, J.; Haskins, P. J. In *Decomposition, Combustion and Detonation Chemistry of Energetic Materials*; Brill, T. B., Russell, T. P., Tao, W. C., Wardle, R. B., Eds.; *Mater. Res. Soc. Symp. Proc.* **1995**, *418*, 267−275.

(37) Aubuchon, C. M.; Rector, K. D.; Holmes, W.; Fayer, M. D. *Chem. Phys. Lett.* **1999**, *200*, 84.

(38) Deak, J. C.; Iwaki, L. K.; Dlott, D. D. *J. Phys. Chem. A* **1999**, *103*, 971.

INTENTIONALLY LEFT BLANK.

NO. OF COPIES	ORGANIZATION
2	DEFENSE TECHNICAL INFORMATION CENTER DTIC DDA 8725 JOHN J KINGMAN RD STE 0944 FT BELVOIR VA 22060-6218
1	HQDA DAMO FDT 400 ARMY PENTAGON WASHINGTON DC 20310-0460
1	OSD OUSD(A&T)/ODDDR&E(R) R J TREW THE PENTAGON WASHINGTON DC 20301-7100
1	DPTY CG FOR RDA US ARMY MATERIEL CMD AMCRDA 5001 EISENHOWER AVE ALEXANDRIA VA 22333-0001
1	INST FOR ADVNCD TCHNLGY THE UNIV OF TEXAS AT AUSTIN PO BOX 202797 AUSTIN TX 78720-2797
1	DARPA B KASPAR 3701 N FAIRFAX DR ARLINGTON VA 22203-1714
1	US MILITARY ACADEMY MATH SCI CTR OF EXCELLENCE MADN MATH MAJ HUBER THAYER HALL WEST POINT NY 10996-1786
1	DIRECTOR US ARMY RESEARCH LAB AMSRL D D R SMITH 2800 POWDER MILL RD ADELPHI MD 20783-1197

NO. OF COPIES	ORGANIZATION
1	DIRECTOR US ARMY RESEARCH LAB AMSRL DD 2800 POWDER MILL RD ADELPHI MD 20783-1197
1	DIRECTOR US ARMY RESEARCH LAB AMSRL CI AI R (RECORDS MGMT) 2800 POWDER MILL RD ADELPHI MD 20783-1145
3	DIRECTOR US ARMY RESEARCH LAB AMSRL CI LL 2800 POWDER MILL RD ADELPHI MD 20783-1145
1	DIRECTOR US ARMY RESEARCH LAB AMSRL CI AP 2800 POWDER MILL RD ADELPHI MD 20783-1197
	ABERDEEN PROVING GROUND
4	DIR USARL AMSRL CI LP (BLDG 305)

NO. OF COPIES	ORGANIZATION
	ABERDEEN PROVING GROUND
22	DIR USARL
	AMSRL WM
	B RINGERS
	AMSRL WM BD
	B E FORCH
	W R ANDERSON
	S W BUNTE
	C F CHABALOWSKI
	A COHEN
	R DANIEL
	D DEVYNCK
	R A FIFER
	B E HOMAN
	A J KOTLAR
	K L MCNESBY
	M MCQUAID
	M S MILLER
	A W MIZIOLEK
	J B MORRIS
	R A PESCE-RODRIGUEZ
	B M RICE
	R C SAUSA
	M A SCHROEDER
	J A VANDERHOFF
	AMSRL WM MB
	B FINK

REPORT DOCUMENTATION PAGE

Form Approved
OMB No. 0704-0188

1. AGENCY USE ONLY *(Leave blank)*	2. REPORT DATE	3. REPORT TYPE AND DATES COVERED
	February 2001	Reprint, Jun 1999–Feb 2000

4. TITLE AND SUBTITLE
Theoretical Studies of Solid Nitromethane

5. FUNDING NUMBERS
622618.H80

6. AUTHOR(S)
Dan C. Sorescue,* Betsy M. Rice, and Donald L. Thompson*

7. PERFORMING ORGANIZATION NAME(S) AND ADDRESS(ES)
U.S. Army Research Laboratory
ATTN: AMSRL-WM-BD
Aberdeen Proving Ground, MD 21005-5066

8. PERFORMING ORGANIZATION REPORT NUMBER
ARL-RP-14

9. SPONSORING/MONITORING AGENCY NAMES(S) AND ADDRESS(ES)

10.SPONSORING/MONITORING AGENCY REPORT NUMBER

11. SUPPLEMENTARY NOTES
* Department of Chemistry, Oklahoma State University, Stillwater, OK 74078
A reprint from the *Journal of Physical Chemistry B*, vol. 104, no. 35, pp. 8406-8419.

12a. DISTRIBUTION/AVAILABILITY STATEMENT
Approved for public release; distribution is unlimited.

12b. DISTRIBUTION CODE

13. ABSTRACT *(Maximum 200 words)*

A classical potential to simulate the dynamics of a nitromethane crystal as a function of temperature and pressure is described. The intramolecular part of the potential was taken as superposition of bond stretching, bond bending, and torsional angles terms. These terms were parametrized on the basis of the geometric and spectroscopic (vibrational frequencies and eigenvectors) data obtained using ab initio molecular orbital calculations performed at the B3LYP/6-31G level on an isolated molecule. The intermolecular potential used is of the Buckingham 6-exp form plus charge-charge Coulombic interactions and has been previously developed by us (Sorescu, D. C.; Rice, B. M.; Thompson, D. L. J. Phys. Chem. 1997, B101, 798) to simulate crystals containing nitramine molecules and several other classes of nitro compounds. The analyses performed using constant pressure and temperature molecular dynamics simulations and molecular packing calculations indicate that the proposed potential model is able to reproduce accurately the changes of the structural crystallographic parameters as functions of temperature or pressure for the entire range of values investigated. In addition, the calculated bulk modulus of nitromethane was found in excellent agreement with the corresponding experimental results. Moreover, it was determined that the present potential predicts correctly an experimentally observed 45° change in methyl group orientation in the high-pressure regime relative to the low-temperature configuration.

14. SUBJECT TERMS
nitromethane, molecular dynamics, intermolecular interaction potential

15. NUMBER OF PAGES
20

16. PRICE CODE

17. SECURITY CLASSIFICATION OF REPORT	18. SECURITY CLASSIFICATION OF THIS PAGE	19. SECURITY CLASSIFICATION OF ABSTRACT	20. LIMITATION OF ABSTRACT
UNCLASSIFIED	UNCLASSIFIED	UNCLASSIFIED	UL

INTENTIONALLY LEFT BLANK.

USER EVALUATION SHEET/CHANGE OF ADDRESS

This Laboratory undertakes a continuing effort to improve the quality of the reports it publishes. Your comments/answers to the items/questions below will aid us in our efforts.

1. ARL Report Number/Author ARL-RP-14 (POC: Rice) Date of Report February 2001

2. Date Report Received _____

3. Does this report satisfy a need? (Comment on purpose, related project, or other area of interest for which the report will be used.) _____

4. Specifically, how is the report being used? (Information source, design data, procedure, source of ideas, etc.) _____

5. Has the information in this report led to any quantitative savings as far as man-hours or dollars saved, operating costs avoided, or efficiencies achieved, etc? If so, please elaborate. _____

6. General Comments. What do you think should be changed to improve future reports? (Indicate changes to organization, technical content, format, etc.) _____

CURRENT ADDRESS

_____
Organization

_____
Name E-mail Name

_____
Street or P.O. Box No.

_____
City, State, Zip Code

7. If indicating a Change of Address or Address Correction, please provide the Current or Correct address above and the Old or Incorrect address below.

OLD ADDRESS

_____
Organization

_____
Name

_____
Street or P.O. Box No.

_____
City, State, Zip Code

(Remove this sheet, fold as indicated, tape closed, and mail.)
(DO NOT STAPLE)

DEPARTMENT OF THE ARMY

OFFICIAL BUSINESS

NO POSTAGE
NECESSARY
IF MAILED
IN THE
UNITED STATES

BUSINESS REPLY MAIL
FIRST CLASS PERMIT NO 0001,APG,MD

POSTAGE WILL BE PAID BY ADDRESSEE

DIRECTOR
US ARMY RESEARCH LABORATORY
ATTN AMSRL WM BD
ABERDEEN PROVING GROUND MD 21005-5066